Proceedings of the ASME 27th International Conference on Offshore Mechanics and Arctic Engineering
OMAE2008
June 15-20, 2008, Estoril, Portugal

OMAE2008-57471

VIV CONTROL AND DRAG REDUCTION USING THE GUIDED POROSITY CONCEPT

Antonio C. Fernandes
COPPE/UFRJ
acfernandes@peno.coppe.ufrj.br

Fabio M. Coelho
COPPE/UFRJ
fmcoelho@peno.coppe.ufrj.br

Ricardo Franciss
CENPES/PETROBRAS
franciss@petrobras.com.br

Severino F. S. Neto
COPPE/UFRJ
severino@peno.coppe.ufrj.br

ABSTRACT

This paper aims to discuss the effectiveness of a new passive kind of VIV (Vortex Induced Vibrations) suppression. Moreover, the proposed solutions leads to a significant drag reduction when compared with conventional proposals (strakes for instance). The concept of guided porosity is applied in experimental tests conducted with low mass ratio cylindrical models. The works also shows that the job (VIV control and drag reduction) is achieved without moving parts, in contrast with segmented fairings. It also advances in terms of the omni-directional solution. Initially, the concept is discussed in terms of the potential theory. Then experimental results are presented in terms of displacements and forces.

INTRODUCTION

The guided porosity is an alternative method for the suppression of vortex induced vibrations (VIV) with drag reduction. This contrasts with strakes, which considerably increase the drag forces acting on cylindrical structures such as risers and spar buoy platforms. Guided Porosity is also a type of passive control of VIV possibly with good economical and operational advantages if compared with active control methods.

The paper focuses on the application of the concept of guided porosity, previously presented by Fernandes [1]. This last reference showed the effectiveness of the concept in air. The present paper shows the effectiveness of the guided porosity in water. For this verification, experiments were carefully designed to be carried out at the current channel of the LOC/COPPE/UFRJ (Laboratório de Ondas e Correntes - Waves and Currents Laboratory of COPPE/UFRJ).

As previously mentioned [1], the basic idea of guided porosity is to allow the flow through the structures (maybe through a outside sleeve in actual applications). The flow is based on the pressure gradient that exists in the flow between the stagnation point region (high pressure) and the separation point region (low pressure). This causes a natural flow that may be used to feed the separation point region which modifies the original vortex generation.

The pressure coefficient, in accordance with potential flow theory is given by Equation 1 [2] and may be used for estimates. For the stagnation point ($\theta = 0$), C_P = *+1* and for $\theta = 90^0$, C_P = *-3*. Considering viscous effects it is known that the actual separation point is about 82^0 for laminar flow and about 120^0 for turbulent flow [2].

$$C_P = 1 - 4\,sen^2\theta \tag{1}$$

Where:

$$C_P = \frac{p - p_\infty}{\frac{1}{2}\rho U_\infty^{\,2}} \tag{2}$$

On the experimental setup, the cylinder was free to move on the direction transversal to the current flow. The top was supported by a bearing system. The bottom was free but with distance small enough (15 mm) to assure two-dimensional flow in most of the cylinder. The data acquisition for displacements was done with an image acquisition system that works with the image contrast between a LED positioned on the top of the system and a dark background provided by a cover during the experiments. For the measurement of the drag coefficient, a

load cell designed for this purpose was placed between the cylinder and the elastic support.

GEOMETRY DEFINITION FROM KINEMATIC BEHAVIOR

As said before, the porosity allowed the flow to enter at the stagnation point region and guided the flow to leave the cylinder near the external separation point region. Basically, the ratio between the entrance and the output areas must be high enough to assure high inflow volume and high outflow velocity.

In order to define the geometry of input and output of the guided porosity device, tests were carried out for three different configurations of the device. For this first purpose, only displacements were measured in order to find out the most effective geometry in the reduction of VIV amplitude.

The results are presented in terms of non dimensional amplitude (*A/D*) for a range of reduced velocity ($V_R=U/f_ND$). The natural frequency is defined in still water. The Reynolds Number ($Re=UD/\nu$) during the tests ranges from $1x10^4$ to $4x10^4$ what indicates that the predicted separation point occurs in fact at an angle of approximately 82^0 from the stagnation point. Three models with 75 mm of diameter (*D*) were tested. The mass ratio $m^*=(m+m_a)/\rho D^2$ of the three models was kept constant and equal to 0.93, where *m* is the oscillating mass, m_a is the added mass and ρ is the water density.

Figures 1-a, 1-b and 1-c illustrate the models 1, 2 and 3, respectively. Note the differences in the input and output areas as explained next.

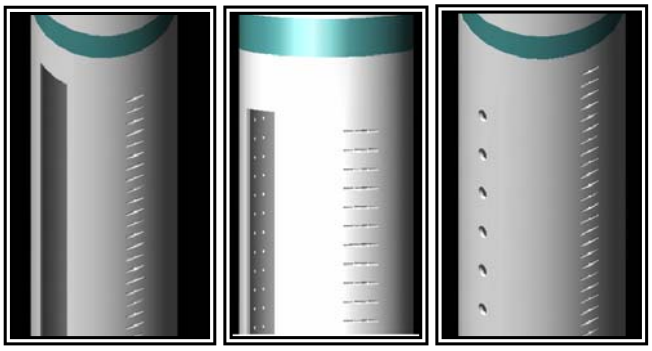

(a) (b) (c)

Figure 1 – (a) Model 1. (b) Model 2. (c) Model 3

The outputs of the three models were designed such that the flow is tangent to the cylinder at this point. The outflow holes are 1 mm in diameter. The three models are different in terms of entrance area, number and position of the outflow holes.

Model 1 inflow is illustrated in Figure 1-a, with 19 mm of width. The outflow holes are positioned at an angle of 70^0 from the stagnation point. The distance between these points is 5 mm. Model 2 is similar to Model 1, except in the outflow. Model 2 has two vertical lines of outflow holes positioned at 70^0 and 80^0 from the stagnation point. Model 3 has an inflow with holes placed 20 mm apart from each other. The diameter of these holes is 5 mm. The outflow consists of holes similar to the first two models, but now, placed at 80^0 from the stagnation point.

Figures 2, 3 and 4 present results for models 1, 2 and 3, respectively. These Figures compare cases with and without the action of the guided porosity. The base case test without porosity for each model was done by simply blocking the outflow holes. As it can be seen in Figure 2, Model 1 working with guided porosity presents a reduction of A/D for a wide range of reduced velocity, except at the peak amplitude, were the results with the model with porosity almost reaches the case without porosity. Note that as previously observed, Model 1 has the outflow placed at 70^0 from the stagnation point.

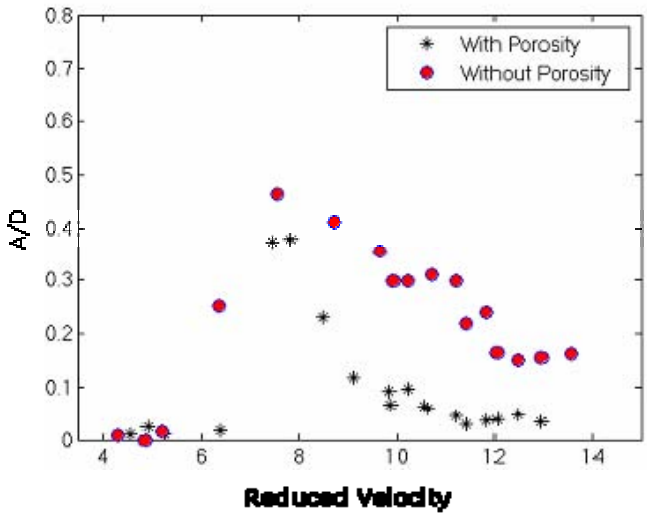

Figure 2 - Relation between A/D and V_R for Model 1, with and without porosity.

Differently from the results of Model 1, Figure 3 presents a significant reduction on the amplitude to diameter ratio response, *A/D*, for any value of reduced velocity obtained from the experiment. Model 2 has two vertical lines of holes placed at 70^0 and 80^0. The entrance is the same as in Model 1 what suggests that the outflows placed near the separation point make a significant difference.

Placement of the outflows near the separation point seems to be the key for the correct operation of the concept. However, Model 2 presented a higher number of outflows than Model 1, and this influence was also investigated. The entrance of models 1 and 2 seems also unfeasible. In order to answer these questions, Model 3 was tested with and without porosity.

Model 3 has the same number of holes as Model 1. These holes are placed at 80^0 from the stagnation point. The entrance shape is like that presented in Figure 1-c, with dimensions as previously described. As can be observed in Figure 4, the reduction on A/D is still very significant for all values of

reduced velocity. It clearly shows that, for laminar flow, the guided porosity design with outflows placed around 80^0 is strongly effective for VIV reduction.

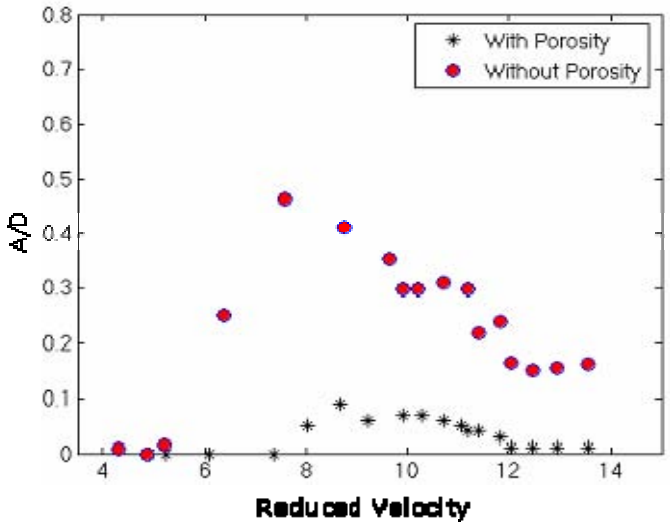

Figure 3- Relation between A/D and V_R for Model 2, with and without porosity.

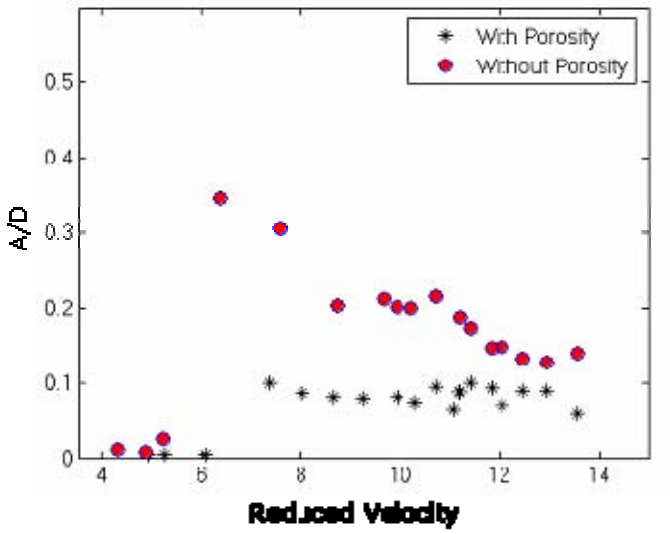

Figure 4- Relation between A/D and V_R for Model 3, with and without porosity.

The maximum non-dimensional amplitude of vibration (*A/D*) for the base cases of Models 1, 2 and 3 was 0.48, 0.48 and 0.35, respectively, and is close to the classical results presented in a summarized form in King (1974) and Williamson (2004) as function of the Stability Parameter ($K_S = 2m^* 2\pi\zeta$) and the Skop-Griffin Parameter ($S_G = 2\pi^3 S^2 m^* \zeta$) (*St* refers to the Strouhal Number). The values of these parameters for the base cases are 4.61 and 0.66, respectively.

INFLUENCE OF THE ANGLE OF UNIFORM FLOW INCIDENCE

In order to evaluate how effective is the device of guided porosity when submitted to different angles of flow incidence from the inflow hole, tests were carried out with a model similar to the previous ones, except by the geometric dimensions. The main objective of these tests is to obtain, in the future, an indication for an effective design of porosity devices distributed helicoidally along the structure.

The inflow holes for this case are 9mm wide and 21mm long squares. The diameter of the outflow holes is 1mm. The holes were distributed over two vertical lines placed at 72^0 and 80^0 from the theoretical stagnation point. The mass ratio is the same as the previous ones ($m^* = 0.93$).

Figure 5 presents results in terms of *A/D* x V_R for the referred model with porosity, for a uniform flow with incidence angle of 0^0. It is also presented the comparison with its base case (without porosity). Similar tests were carried out for the same model submitted to uniform flow incidence angles of 30, 60, 90, 120, 150 and 180 degrees from the inflow holes of the porosity device. The peak amplitudes of vibration (A/D_{max}) for each of these cases are presented in Figure 6. The blue line represents the base case.

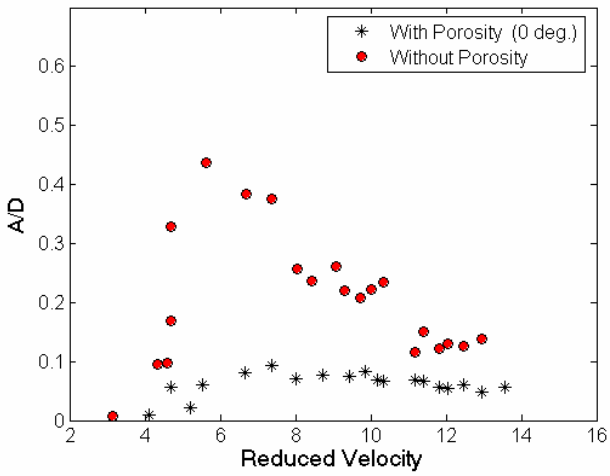

Figure5 - *A/D* x V_R for a 0^0 incidence of the uniform flow.

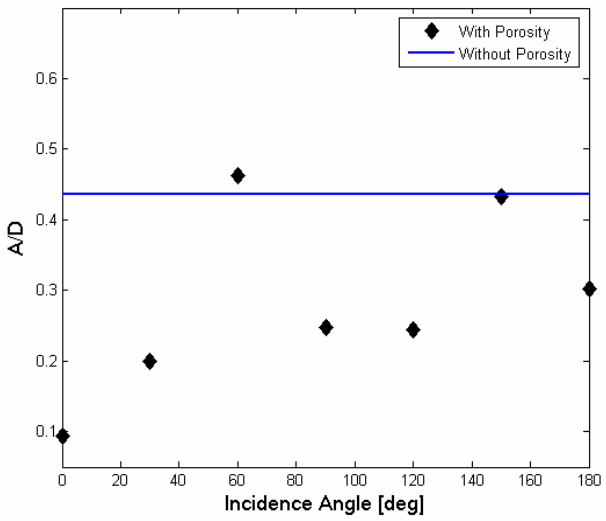

Figure 6- A/D_{max} for each uniform flow incidence angle, measured from the inflow holes of the porosity device.

It can be inferred that the guided porosity tends to be effective not only for flow incidence in the direction of the inflow holes, but also for 30^0, 90^0 and 120^0 from the inflow holes, presenting a 50 percent of reduction in these directions. For 180^0, it is also effective, presenting 40 percent of reduction. It is important to note that for 60^0 and 150^0 from the inflow holes, the guided porosity does not reduce neither amplifies the vibration amplitude, what is positive for design purpose. These test results will serve as a basis towards a future design aiming at omni-directionality.

DRAG EVALUATION FOR STATIONARY AND OSCILLATORY MODELS

Effects on drag forces were also focused. A large drag reduction has been observed. This is certainly an additional feature of the guided porosity device. The tests with force measurements were carried out for three models: smooth cylinder, cylinder with strakes and cylinder with porosity. Firstly, the tests were conducted for a fixed cylinder to get comparisons with the literature. Later, the cylinders were allowed to move transversally while the drag was measured.

The models were assembled such that the distance between their lower extremity and current channel bottom was 15 mm. The mass ratios for the smooth model, the model with porosity and the model with strakes were, respectively, 1.04, 1.09 and 1.09. Figures 7 and 8 present pictures of the models with porosity and strakes. The diameter of the models is 75 mm. The model with porosity is the same presented in the previous section. The strakes of the third model were distributed in three segments, having 0.25D width, 25D pitch, and separated by 120^0.

Figure 7- Model with porosity.

Figure 8- Model with strakes.

Figure 9 presents comparisons for the two referred stationary models and the smooth cylinder in terms of Drag Coefficient, for a range of Reynolds Number.

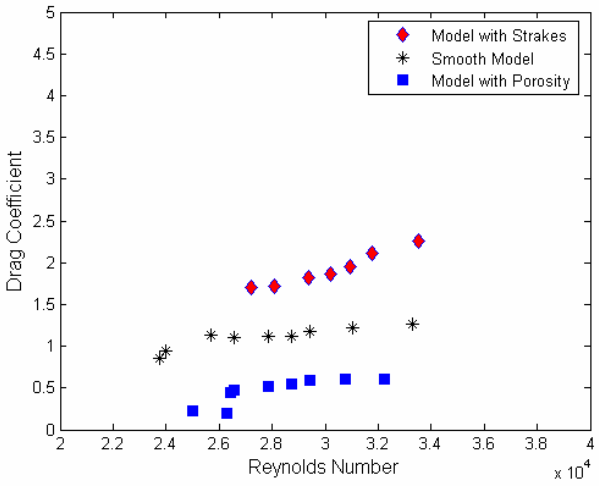

Figure 9 - Comparison between the C_D for the three referred stationary models.

It can be observed from this result that the model with porosity presents a smaller drag coefficient (around 0.6) in comparison with the smooth cylinder (around 1.1). The model with strakes increase significantly the drag coefficient (around 2.1) as expected. It can be concluded that the guided porosity also is highly effective in reducing the cylinder drag coefficient, specially, in comparison with strakes.

The tests with the porosity model free to move in the transverse direction are presented in Figures 10 and 11. From Figure 10, it can be seen that the VIV amplitude of the model with porosity is much lower than its base case as shown in the previous sections.

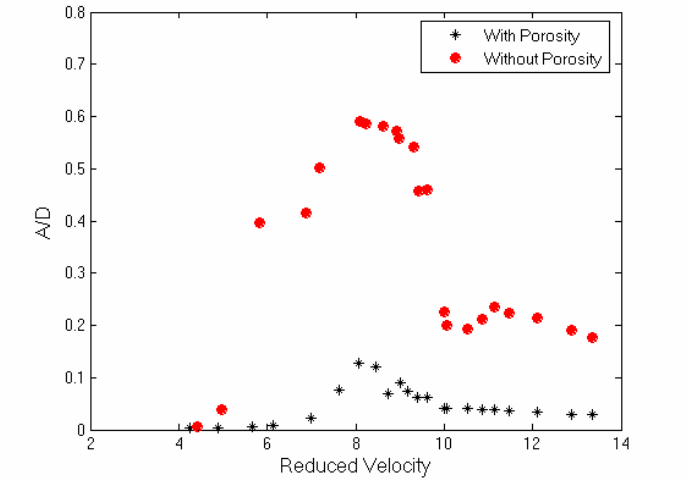

Figure 10 - Comparisons in terms of *A/D* x V_R between the model with porosity and its base case, both free to move in transverse direction.

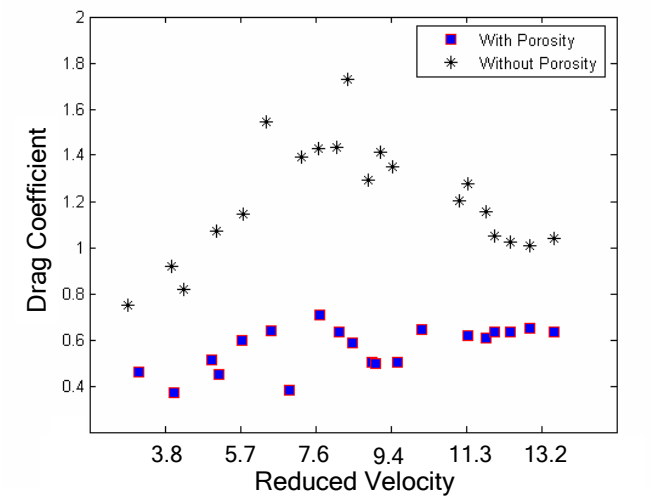

Figure 11- Comparison between the C_D for the model with porosity and its base case.

From Figure 11, it is clear that the drag coefficient for the base case has an increasing due to the VIV amplitude. On the other hand, the model with porosity presented almost no drag increasing in accordance with its small VIV amplitude.

ADVANCES IN THE OMNI-DIRECTIONAL SOLUTION

The present work, based on the study of the variations on the angle of incident flow, propose an omni-directional solution. The model proposed has a 14D of pitch. The pitch in this case refers to the angular evolution of the inflow holes along the spam of the cylinder, as well as the outflow holes. The width of each porosity module is 5 cm. Figure 12 presents a picture of the referred model. The inflow and outflow holes have the same properties presented on the investigation about the angle of incident flow.

Figure 12 – Model proposed as omni-directional solution.

The figures 13 to 18 present the results in terms of displacements for this proposed model in comparison to the case without porosity. Once the cylinder has no sufficient length to reach one complete pitch, tests were conducted for different angles of flow incidence. This angle has the reference on the inlet hole of the highest module.

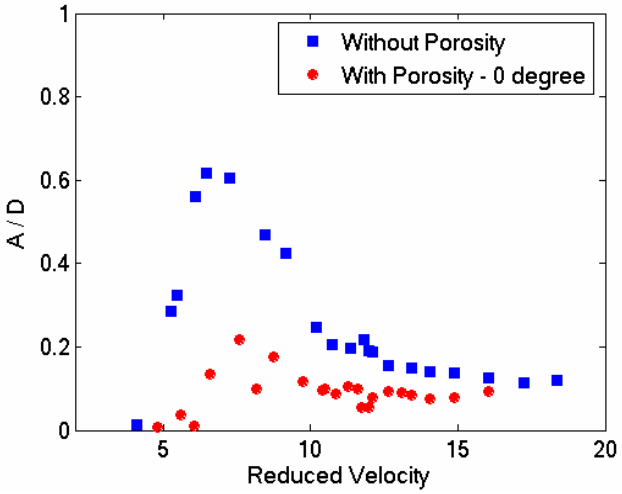

Figure 13 – Displacements for the proposed model on 0º.

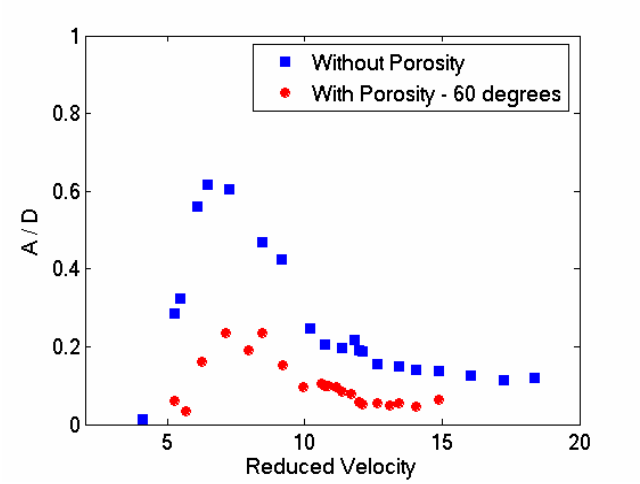

Figure 14 – Displacements for the proposed model on 60º.

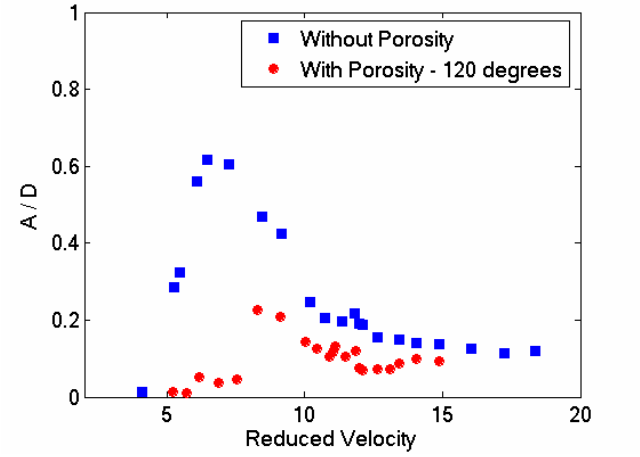

Figure 15 – Displacements for the proposed model on 120º.

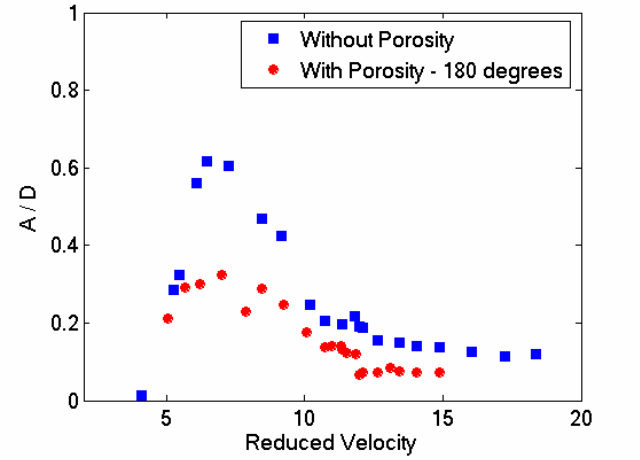

Figure 16 – Displacements for the proposed model on 180º.

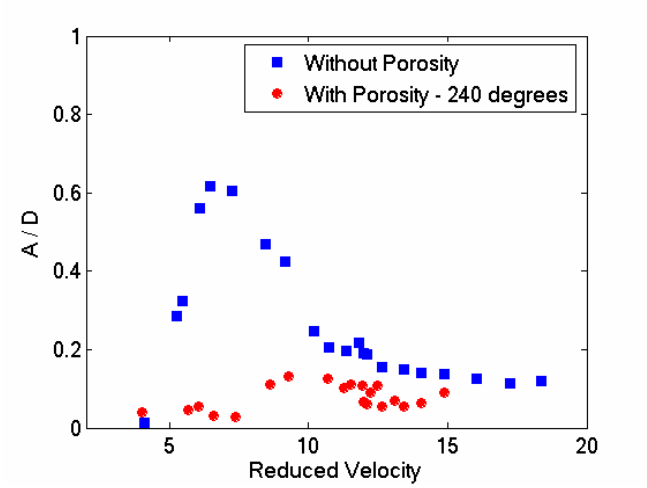

Figure 17 – Displacements for the proposed model on 240º.

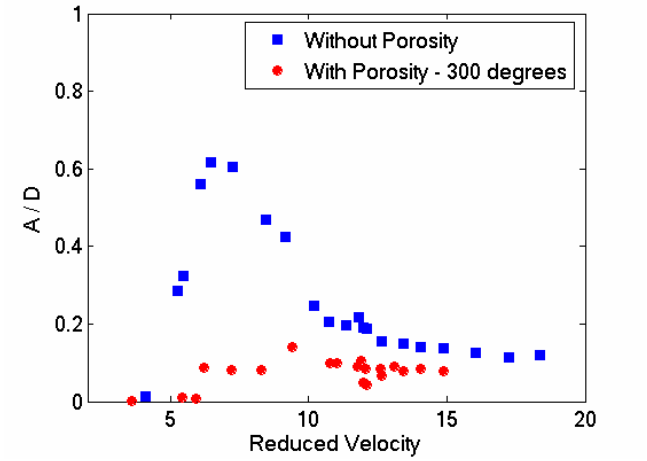

Figure 18 –Displacements for the proposed model on 300º.

As it can be observed from the results, in terms of displacements, the proposed solution has shown to be very effective in reducing VIV. Only kinematics was investigated, once the proposed solution still must be improved in terms pitch and inflow / outflow areas. For this purpose the kinematics study is very interesting and gives a good idea about the potentiality of the model even in terms of drag reduction

CONCLUSIONS

The present work shows clear evidences of the effectiveness of the concept of guided porosity in terms of both VIV reduction, and drag reduction, by means of experimental tests with rigid cylinders. The guided porosity concept presents much lower drag coefficients (around 0.6), than those common industry solutions which use strakes, as the one adopted in the present paper (three segments of 0.25D width, 25D pitch, separated by 1200). The strake solution presented a drag coefficient around 2.1. A consequence of the drag reduction (3.5 times !) would be a reduction of line overall diameter and

also an increase of its fatigue service life. Both may lead to substantial economic savings.

Variations on the angle of flow incidence, measured from the inflow pores allowed observing that the guided porosity is also effective in flow directions different from the inflow pores direction. It can lead to an omni-directional solution for risers and spar platforms.

The omni-directionality proposed here is also effective in reducing VIV and gives a good perspective in terms of finding the best arrangements for the porosity distribution.

ACKNOWLEDGMENTS

The authors would like to thank PETROBRAS for the financial support given to this work, and LOC/COPPE/UFRJ team (Laboratory of Waves and Currents from COPPE/UFRJ) for the experiments. The PRH-ANP (Human Resources Program of Brazilian Petroleum Agency) is also acknowledged. The first author acknowledges CNPq (The Brazilian Research Council). And finally, special thanks are given to the team of LEME/COPPE/UFRJ for the professionalism and dedication in the development of the load cell and acquisition system for force measurements.

REFERENCES

[1] Fernandes, A.C., Esperança, P.T.T., Sphaier, S.H. and Silva, R.M.C.; VIV Mitigation: Why not Porosity; XIX International Symposium on Offshore Mechanics and Arctic Engineering (ETCE/OMAE2000 Joint Conference); New Orleans, Estados Unidos, February 14-17, 2000.

[2] White, F.K.; Fluid Mechanics; New York, WCB/McGraw-Hill, 1999.

[3] King, R. Vortex Excited Structural Oscillations of a Circular Cylinder in Flowing Water, Ph.D. Thesis, Laoghbororough University of Technology, U.K., 1974.

[4] Williamson C.H.K. and Govardhan, R. ; Vortex Induced Vibrations ; Annual Review on Fluid Mechanics, 2004.